Analysis of the Performance of Thermoelectric Generators for Ambient Energy Generation through ANSYS Software

Saleh, Umar Abubakar
Faculty of Electrical and Electronics Engineering, Universiti Tun Hussein Onn Malaysia, Johor, Malaysia.
Centre for Atmospheric Research, National Space Research and Development Agency, Prince Audu Abubakar University Anyigba, Kogi, Nigeria.
abubakarumarsaleh1982@gmail.com

S. A. Jumaat
Faculty of Electrical and Electronics Engineering, Universiti Tun Hussein Onn Malaysia, Johor, Malaysia
amely@uthm.edu.my

Johar Muhammad Akmal & W. A. W. Jamaludin
Faculty of Mechanical and Manufacturing Engineering, Universiti Tun Hussein Onn Malaysia Johor, Malaysia
akmal@uthm.edu.my
wan.akashah.kromme@gmail.com

Abstract

The continued growth in fossil fuel price and their negative environmental impact have forced scientists to look inward for an alternative energy source. This paper analyzed the Performance of Thermoelectric Generators for Ambient Energy Generation. Thermoelectric generators (TEG) are bi-directional modules used as coolant and energy generators and has a wide range of application. The simulation technique is one of the best options to evaluate thermoelectric generators' performance for ambient energy generation. This paper presents the designed and evaluation of the TEG as ambient sources using ANSYS software. The results indicate that the TEG can convert excess heat to electrical energy whenever there is a temperature gradient across the hot side and the cold side of TEG. The results show that one TEG unit can generate a 1.5800×10^{-4} Watt of power.

Keyword
Thermoelectric Generators, Ambient Energy, ANSYS Software,

1 Introduction

One of the big problems facing humanity soon is the increase in greenhouse emissions and minimizing its impact on the environment (Ahsan, 2020). At the same time, energy needs are rising daily (Elghool et al., 2020; Saleh et al., 2018; Saleh et al., 2015). The recovery of lost thermal energy for conversion to electricity is a significant challenge for researchers and the industry (Miao et al., 2020). TEGs will contribute to this initiative. As a growing, environmentally friendly source of ambient energy harvesting primarily through waste heat via temperature gradients, a thermoelectric generator may be the prospect of meeting energy challenges in the coming generation. (Kishore et al., 2020). A solid-state system is referred to as a thermo-electric generator using the Seebeck effect to generate electricity Thomas Johann Seebeck first detected thermo-electric phenomena in 1821. He observed

the compass magnet's deflection whenever there is a temperature gradient between two dissimilar materials' junctions. (Chintha, 2019). Indeed, such deflection is the electrical current output caused by the closed-loop described by the Ampere law. (Hussain & Muhammad, 2020). The closed circuit's driving current is the potential difference between hot and cold junctions for the generation of temperature gradients called the "Seebeck effect." The potential difference has a direct correlation with the temperature difference. (Marchenko, 2020). An intrinsic thermoelectric material property expressed in the equation (1) is the Seebeck coefficient

$$\alpha = \frac{\Delta V}{\Delta T} \quad (1)$$

where ΔV, ΔT and α are the voltage produced, the temperature gradient and the Seebeck coefficient in the system (Hussain & Muhammad, 2020). This paper, therefore, presents the simulation of TEG for Ambient energy generation using Ansys simulation software.

2 Thermoelectric Generator

Thermoelectric generators as power generation are divided into two groups, namely, high power generation and low power generation (Cekdin et al., 2020; Saleh et al., 2020). TEG development for low power is investigated through an environmentally friendly and cost-effective method known as direct ink. (Shakeel et al., 2020). The TEGs were produced on a glass substrate, the most popular insulator used in houses, and windows of two different sizes were made of poly (3, 4- ethylene dioxythiophene) polystyrene sulfonate (PEDOT: PSS) ink and silver ink materials. For TEGs with varying lengths of 30 and 40 mm at a temperature difference of 120 ºC, the results indicate a maximum power of 5.17 ± 0.5 nW and 4.08 ± 0.5 nW. According to (Hamid et al., 2014), TEG can generate power from 5 μW to 1 W with low power generation, while high power generation is considered 1 W and above. Biomedical, remote and aerospace, TEG is used for a low-power generator (Rana et al., 2017). Electronics devices integrated into other bodies using TEG technology for power production are classified under mobile communications. These comprise smartphones, iPods, tablets and media players. Simultaneously, others used are in the medical sector, including hearing aids and heart pacemakers. Electronics devices incorporated in other objects have power specifications of 5 μW to 1 W (Hamid et al., 2014). (Lineykin et al., 2020) presented the development and optimization of a low-temperature difference thermoelectric power harvester for the wireless sensor nodes on water pipelines. The thermoelectric harvester modelling, design, optimization, integration and experimental analysis to replace a 20 Ah battery for a wireless water quality sensor located on a water pipe was done by (Lineykin et al., 2020) using a MATLAB software. The results indicate that the thermoelectric harvester generates more than 0.5-2 mW at a temperature gradient of around 1-2 K at a wind speed of about 1 m/s between the pipe surface and the ambient air.

2.1 Application of Thermoelectric Generator

In a wide range of applications, TEG is used in areas likes wireless sensor network (Lineykin et al., 2020; Yuan et al., 2020) micropower generation (Wen et al., 2020), space power (Wang et al., 2020) automotive waste heat recovery(Krishna et al., 2020; Patel & Patel, 2020). Also, it can be used in wearable sensors (Lund et al., 2020; Umar Abubakar Saleh et al., 2021; U. A. Saleh, M. A. Johar, S. A. Jumaat, M. N. Rejab, 2020), A thermoelectric device is used as a means of cooling electronics equipment (Cai et al., 2019), and also in refrigerators and air conditioning systems (Khanmohammadi et al., 2020; Rostamzadeh & Nourani, 2019). Specific applications for aeronautics, military, medicine, instruments, biological weapon, and other industrial products (Aljaghtham & Celik, 2020; Mirzakhanyan, 2005) and buildings (Al Musleh et al., 2020; Cai et al., 2020)

2.2 Fundamental Equations for Thermoelectric Energy Conversion

Figure 1 presents the schematic diagram of the thermoelectric generator system. The system consists of a TEG hot side attached to the shingle's backside and a heatsink placed at the cold side of the TEG. Figure 2 shows its equivalent circuit diagram with a load resistance R2 connected across the terminal.

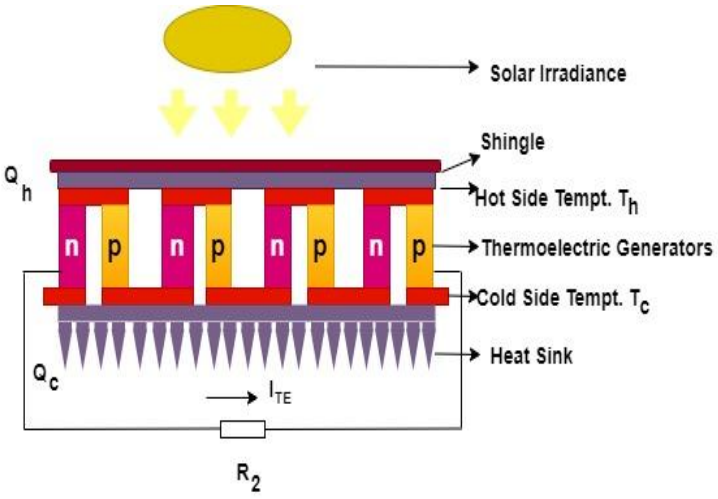

Figure 1. Schematic Diagram of Thermoelectric Generator System

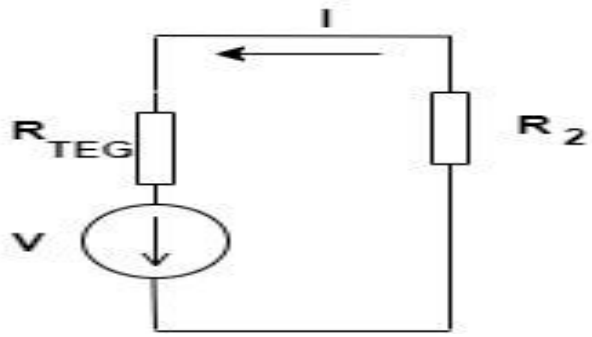

Figure 2. Equivalent Thermoelectric Generator Circuit

The voltage V through the load resistance R_2 is in equation (2)

$$\boldsymbol{V_2 = IR_2 = V - IR_{TEG}} \quad \textbf{(2)}$$

Where: R_{TEG} and I, are the internal resistance of the TEG and the current through the resistance. The current (I) is obtained in equation (3)

$$\mathbf{I} = \frac{\alpha(T_h - T_c)}{R + R_2} \quad \textbf{(3)}$$

Equation (4) and (5) shows the TEG output power

$$\boldsymbol{P = IV = \frac{\alpha^2}{(R_{TEG} + R_2)} \Delta T^2 R_{TEG}} \quad \textbf{(4)}$$

$$\mathbf{P} = \boldsymbol{Q_h - Q_c} \quad \textbf{(5)}$$

Where P is the difference between the thermal energy from the hot side to the cold side of the TEG [37]

$$\boldsymbol{Q_h = \alpha T_h I + K(T_h - T_c) - \frac{1}{2} I^2 R} \quad \textbf{(6)}$$

$$\boldsymbol{Q_c = \alpha T_c I + K(T_h - T_c) - \frac{1}{2} I^2 R} \quad \textbf{(7)}$$

Where$Q_h, Q_c, T_h, and\ T_c$ are the thermal energy of the TEG hot side and cold side to the heat sink, hot side and cold side temperature of the TEG (Sahin et al., 2020)

Equation 8 to 13 give the Polynomial representations for temperature-dependent properties of air and copper and temperature-dependent for the thermoelectric characteristics of n-type and p-type

$$\boldsymbol{K_n = 0.0000334545T^2 - 0.023350303T + 5.606333} \quad \textbf{(8)}$$

$$\boldsymbol{\rho_n = (0.015601732T^2 - 15.708052T + 4466.38095)\ e^2} \quad \textbf{(9)}$$

$$\boldsymbol{\alpha_n = (0.001530736T^2 - 1.08058874T - 28.338095e^{-6}} \quad \textbf{(10)}$$

Where Kn, ρn and αn from equation 8 to 10 are the thermal conductivity, electrical resistivity and Seebeck coefficient of the n-type semiconductor material of the TEG (Barry et al., 2016)

$$\boldsymbol{K_p = 0.0000361558T^2 - 0.026351342T + 6.22162} \quad \textbf{(11)}$$

$$\boldsymbol{\rho_p = (0.01057143T^2 - 10.16048T + 3113.71429)\ e^2} \quad \textbf{(12)}$$

$$\boldsymbol{\alpha_p = (-0.003638095T^2 + 2.74380952T - 296.214286)\ e^{-6}} \quad \textbf{(13)}$$

Where K_p ρ_p and α_p from equation 11 to 13 are the thermal conductivity, electrical resistivity and Seebeck coefficient of the p-type semiconductor material of the TEG (Barry et al., 2016)

3 Methodology

The TEG performance was evaluated using ANSYS simulation software. The software was used for the electromagnetic, thermal, and thermoelectric thermal analysis. The TEG steady-state evaluation, which enables the system's geometric modelling and several simulations inside the TEG module, including current density, temperature distribution, electric voltage, and heat flow, was carried out via ANSYS Workbench. The simulation involves three fundamental processes this consist of the following phases: Pre-processing, Solving and Post-processing. The Pre-processing phase consists of five stages:

1. Modelling of the 3D using the ANSYS Modeller to construct the model geometry (Figure. 3)
2. Selecting of the Thermal-electric for TEG modelling
3. Inputting of the TEG engineering data
4. The building of a solid-state model that allows filed temperature evaluation
5. Generation of the net finite element by ANSYS Meshing (Figure. 4)

Based on direct TEG measurements, the engineering data from the experimental findings and the datasheet, the contact and ceramic substrates' parameters from the ANSYS library. The 3D model was developed, and the thermal boundary conditions were kept constant on the substrates T_h and T_c

Fig.3 is the graphical presentation of the thermoelectric generator with two terminals. The entire structure is created by copper alloy and a p-type portion with thermal conductivity, isotropic resistance and Seebeck coefficient based on equations 8 to 13. The thermal-to-electrical power conversion efficiency of the TE material is scientifically dependent on the following crucial materials properties: the Seebeck coefficient, the electrical

conductivity and thermal conductivity, which are expressed collectively in terms of a dimensionless figure-of-merit.(Kishore et al., 2020)

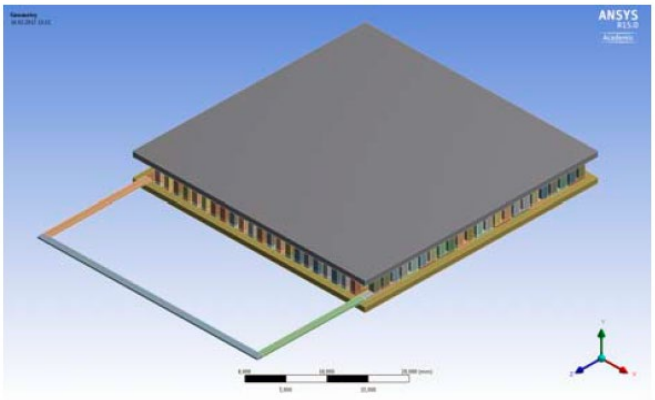

Figure 3. Thermoelectric Generator 3D Model

Fig.4 shows the meshing of the developed TEG at ANSYS. Via mesh, the entire body is divided into the number of parts to distribute the load evenly if any load is applied and automatically selects the necessary mesh in ANSYS for efficiently carrying out the built system's simulation.

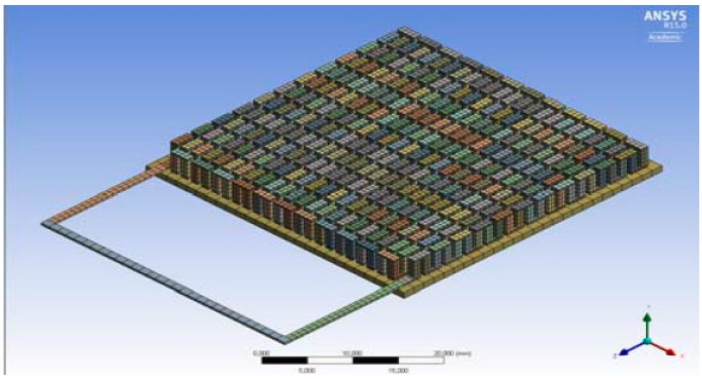

Figure 4. The Finite element Model of the TEG

Figure 5 illustrate the various inputted boundary conditions. The conditions are the shingle hot side temperature as 42 ºC, TEG hot side temperature as 41.5 0 C, TEG cold side temperature as 39.5 ºC and the low potentials been 0V.

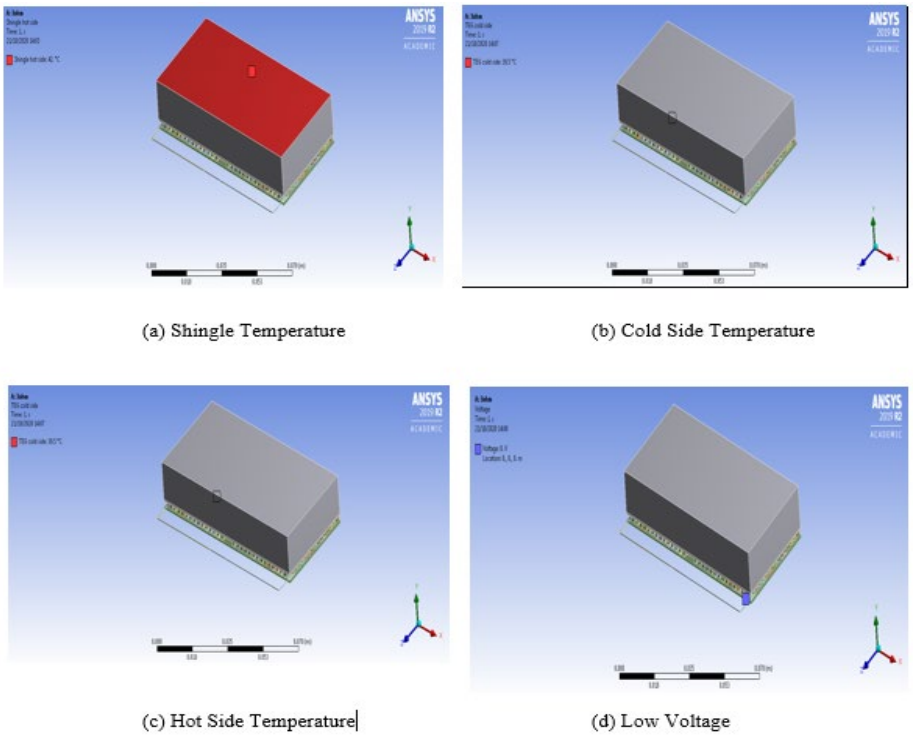

Figure 5. Inputted Boundary Conditions, (a) the Shingle Temperature, (b) Cold and (c) Hot Side Temperature, (d) Low Voltage

4 Result and Discussions

This section discussed the results of the ANSYS simulation of the thermoelectric generator

4.1 Results of ANYSY Simulation

For the TEG performance, this section presents the research results of the ANSYS simulation. Figure 6 shows the temperature profile of the TEG module. The red and blue colour areas indicate higher temperatures and lower temperatures, respectively. As a result, the hot junction has such a higher temperature, and the cold side junction has a lower temperature. The maximum temperature is 27.575 °C, while the minimum temperature is 26.109 °C

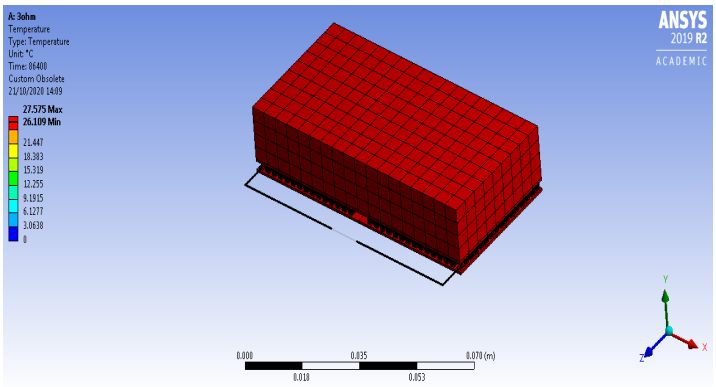

Figure 6. The temperature profile of the designed TEG

The current density across the entire TEG unit is shown in Figure.7, with a minimum current density of 3.076 A/m2, with a maximum density of 1730 A/m2. Essentially, the electron flows from the n-type to the p-type element. As the temperature gradient changes between hot and cold junctions, the current density also significantly changed.

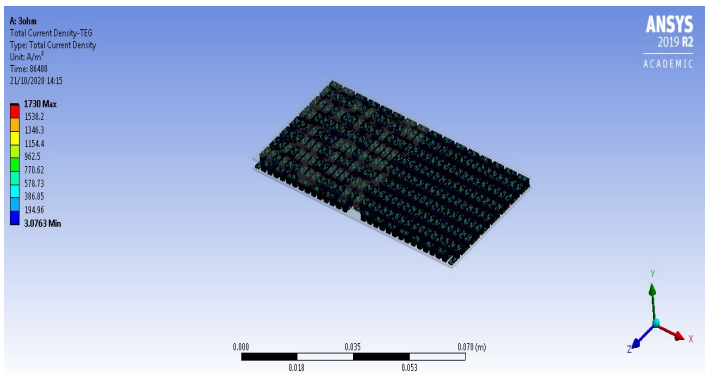

Figure 7. Current Density of the designed TEG

Figure.8 depict the voltage across TEG, which is as a result of the temperature gradient between the hot and cold side of the TEG.

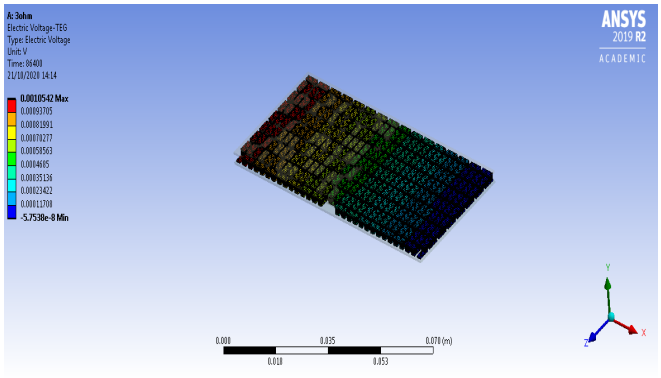

Figure 8. The voltage of the designed TEG

4.2 Results of Temperature Profile and the Power Output

The figures below illustrated the TEG temperature profile and the output power via the Ansys simulation. The results also discussed the effect of the TEG load resistance extensively.

Figure 9 depicts the hot and cold junction temperature Profile of the TEG variation for April 2020, for the hot side, the temperature varies with an increase in the solar irradiance. At midnight the temperature was observed to be 27.745 ºC it maintained the same pattern till around 8 am where it started going up with an increase in the sunshine. The result also shows a maximum temperature of 41.15 ºC at around 1 pm, which resulted from high solar irradiance. The hot side is attached directly to the shingle. As the solar irradiance drop, the temperature also dropped. For the cold side, the temperature also fluctuates with the increase in the irradiance but a heatsink attached to the cold side provide cooling for the cold side to achieve a high-temperature difference between the hot and cold side.

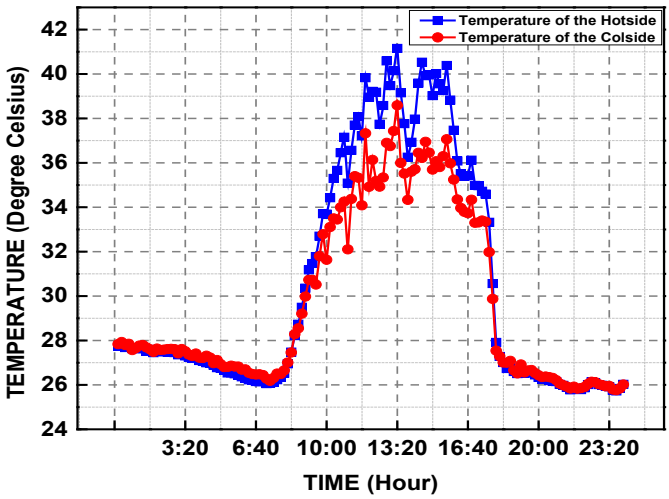

Figure 9 the variation of the hot side temperature and the cold side temperature of the TEG

Figure 10 illustrates the delta T of the TEG for April. The variation was at three intervals in the day as night, morning and afternoon. During the night time, 2:10 am to 9:30 am; the system achieved a temperature difference of 0.01309 ◦C to 0.9210 ◦C. During the morning from 9:40 am to 5:30 pm a temperature difference of 0.9210 ◦C to 1.344 ◦C was reached and during the afternoon between 5:30 pm to 12 am, the system achieve a temperature difference of 1.344 ◦C to 0.0202 ◦C respectively. A maximum delta T of 4.043 ◦C was achieved at 11:50 am.

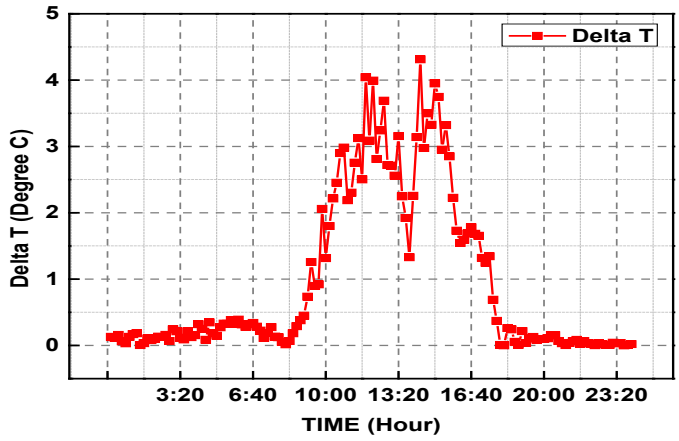

Figure 10. TEG Temperature difference (ΔT)

4.3 Results of Voltage

Figure 11 shows the voltage variations with an increase in the temperature over hourly for 24hours time interval. The voltage measurement range was classified into three times as during the night, morning, and evening time for the TEG temperature changes for Seebeck coefficient. At night, the minimum voltage occurred when delta T is less than one ($0.13^{O}C$) was midnight (2.2660×10^{-3} V), at precisely 06:50 in the morning when delta T was ($0.28^{O}C$) the TEG produced a maximum voltage of 1.77×10^{-2} V. During the day at 12:10 with delta T greater than one ($4.3^{O}C$), the TEG has a maximum voltage of (1.3673×10^{-1}V) it maintains that pattern till around 17:40 the voltage change to be (1.3176×10^{-1}V) and the delta was ($0.69\ ^{O}C$)

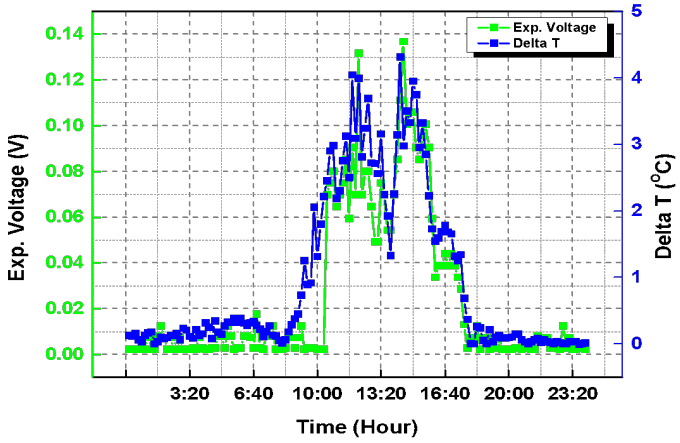

Figure 11. Output Power of TEGs

4.4 Results of Power

Figure 12 depicts the variation was divided into three times in a day as night, morning and afternoon of April 2020. During the night, the results show an output power of 4.2936 x 10^{-9} W to 2.4532 x 10^{-6} W at 12:10 am to 9:30 am. During the morning from 9:40 am to 5:30 pm an output power of 8.5685 x 10^{-7} W to 1.5800 x 10^{-4} W was reached and during the afternoon between 5:30 pm to 12 am, the result shows an output power of 9.1892 x 10^{-9} W to 1.3545x 10^{-6} W were achieved, respectively. Maximum power output was obtained at 11:50 am.

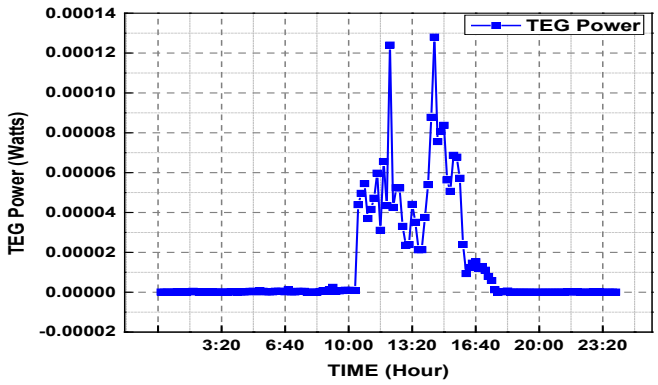

Figure 12. Output Power of TEGs.

Figure 13 shows the variation of the output power to the load. Based on the graph, the optimal power occurred at a load of 3 ohms. The results show that the load resistance is equal to the number of p and n-type semiconductor legs, equivalent to the internal electrical resistance.

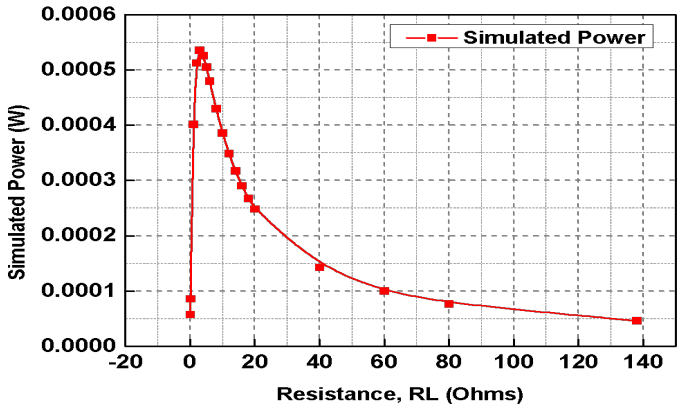

Figure 13: Variation of the TEG Simulated Output Power and the Load Resistance R_2

5 Conclusion

The simulation results have shown the practical approach to TEG physics research. In particular, it allows the efficient use of TEG as a cooling device and ambient energy generators. It will also play a significant role in hybrid system formation with photovoltaic panels for improved energy generation and increase its lifespan. It will lead to the TEGs in large scale production to the end-user in terms of power and temperatures at the specified load resistance.

Acknowledgements

The research was mainly supported by Ministry of Higher Education (MOHE) through Fundamental Research Grant Scheme (FRGS/1/2018/TK10/UTHM/02/2) or Vot No. K108.

Reference

Ahsan, N., Solar panel size for a single-family house. *Proceedings of the International Conference on Industrial Engineering and Operations Management*, *August*, 2694–2699, 2020.

Al Musleh, M., Topriska, E. V., Jenkins, D., & Owens, E., Thermoelectric generator characterization at extra-low-temperature difference for building applications in extreme hot climates: Experimental and numerical study. *Energy and Buildings*, vol. *225*, pp. 110285, 2020. https://doi.org/10.1016/j.enbuild.2020.110285.

Aljaghtham, M., & Celik, E., Design optimization of oil pan thermoelectric generator to recover waste heat from internal combustion engines. *Energy*, vol. *200*, pp. 117547, 2020. https://doi.org/10.1016/j.energy.2020.117547

Barry, M. M., Agbim, K. A., Rao, P., Clifford, C. E., Reddy, B. V. K., & Chyu, M. K., Geometric optimization of thermoelectric elements for maximum efficiency and power output. *Energy*, vol. *112*, pp. 388–407, 2016. https://doi.org/10.1016/j.energy.2016.05.048

Cai, Y., Wang, W. W., Liu, C. W., Ding, W. T., Liu, D., & Zhao, F. Y., Performance evaluation of a thermoelectric ventilation system driven by the concentrated photovoltaic thermoelectric generators for green building operations. *Renewable Energy*, vol. *147*, pp. 1565–1583, 2020. https://doi.org/10.1016/j.renene.2019.09.090

Cai, Y., Wang, Y., Liu, D., & Zhao, F. Y., Thermoelectric cooling technology applied in the field of electronic devices: Updated review on the parametric investigations and model developments. *Applied Thermal*

Engineering, vol. *148*, pp. 238–255, 2019. https://doi.org/10.1016/j.applthermaleng.2018.11.014

Cekdin, C., Nawawi, Z., & Faizal, M., The usage of thermoelectric generator as a renewable energy source. *Telkomnika (Telecommunication Computing Electronics and Control)*, vol. *18*(4), pp. 2186–2192 2020. https://doi.org/10.12928/TELKOMNIKA.V18I4.13072

Chintha, S., *EXPERIMENTAL INVESTIGATIONS ON THERMO ELECTRIC POWER GENERATION FROM WASTAGE*. *XI*(Xii), 90–93 2019.

Elghool, A., Basrawi, F., Ibrahim, T. K., Ibrahim, H., Ishak, M., Hazwan bin Yusof, M., & Bagaber, S. A., Multi-objective optimization to enhance the performance of thermo-electric generator combined with heat pipe-heat sink under forced convection. *Energy*, vol. *208*, pp. 118270, 2020. https://doi.org/10.1016/j.energy.2020.118270

Hamid Elsheikh, M., Shnawah, D. A., Sabri, M. F. M., Said, S. B. M., Haji Hassan, M., Ali Bashir, M. B., & Mohamad, M., A review on thermoelectric renewable energy: Principle parameters that affect their performance. *Renewable and Sustainable Energy Reviews*, vol. *30*, pp. 337–355, 2014. https://doi.org/10.1016/j.rser.2013.10.027

Hussain Shah, W., & Muhammad Khan, W., Thermoelectric Properties of Chalcogenide System. *Electromagnetic Field Radiation in Matter*, vol.1, pp. 1–20, 2020. https://doi.org/10.5772/intechopen.93248

Khanmohammadi, S., Musharavati, F., Kizilkan, O., & Duc Nguyen, D., Proposal of a new parabolic solar collector assisted power-refrigeration system integrated with thermoelectric generator using 3E analyses: Energy, exergy, and exergo-economic. *Energy Conversion and Management*, vol. *220*, pp. 113055, 2020. https://doi.org/10.1016/j.enconman.2020.113055

Kishore, R. A., Nozariasbmarz, A., Poudel, B., & Priya, S., High-Performance Thermoelectric Generators for Field Deployments. *ACS Applied Materials and Interfaces*, vol. *12*(9), pp. 10389–10401, 2020. https://doi.org/10.1021/acsami.9b21299

Krishna Kumar, T. S., Anil Kumar, S., Kodanda Ram, K., Raj Goli, K., & Siva Prasad, V., Analysis of thermo electric generators in automobile applications. *Materials Today: Proceedings*, *xxxx*., 2020. https://doi.org/10.1016/j.matpr.2020.08.081

Lineykin, S., Sitbon, M., & Kuperman, A., Design and optimization of low-temperature gradient thermoelectric harvester for wireless sensor network node on water pipelines. *Applied Energy*, *November*, pp. 116240, 2020. https://doi.org/10.1016/j.apenergy.2020.116240

Lund, A., Tian, Y., Darabi, S., & Müller, C., A polymer-based textile thermoelectric generator for wearable energy harvesting. *Journal of Power Sources*, vol. *480*, pp. 228836, 2020. https://doi.org/10.1016/j.jpowsour.2020.228836

Marchenko, O. Energy and economic analysis of thermoelectric generator on wood fuel. *E3S Web of Conferences*, vol. *209*, pp. 03017, 2020. https://doi.org/10.1051/e3sconf/202020903017

Miao, Z., Meng, X., Zhou, S., & Zhu, M., Thermo-mechanical analysis on thermoelectric legs arrangement of thermoelectric modules. *Renewable Energy*, vol. *147*, pp. 2272–2278, 2020. https://doi.org/10.1016/j.renene.2019.10.016

Mirzakhanyan, A., Economic and social development. *The Armenians: Past and Present in the Making of National Identity*, vol. *3*, pp. 196–210, 2005. https://doi.org/10.4324/9780203004937

Patel, V. R., & Patel, M. C., Automobile Waste Heat Recovery System Using Thermoelectric Generator. *Journal of Science and Technology*, vol. *5*(3), pp. 58–61, 2020. https://doi.org/10.46243/jst.2020.v5.i3.pp58-61

Rana, S., Orr, B., Iqbal, A., Ding, L. C., Akbarzadeh, A., & Date, A., Modelling and Optimization of Low-temperature Waste Heat Thermoelectric Generator System. *Energy Procedia*, vol. *110*, pp. 196–201, 2017. https://doi.org/10.1016/j.egypro.2017.03.127

Rostamzadeh, H., & Nourani, P., Investigating potential benefits of a salinity gradient solar pond for ejector refrigeration cycle coupled with a thermoelectric generator. *Energy*, vol. *172*, pp. 675–690, 2019. https://doi.org/10.1016/j.energy.2019.01.167

Sahin, A. Z., Ismaila, K. G., Yilbas, B. S., & Al-Sharafi, A., A review on the performance of

photovoltaic/thermoelectric hybrid generators. *International Journal of Energy Research*, pp. 1–30, *December 2019*.. https://doi.org/10.1002/er.5139

Saleh, U. A., Haruna, Y. S., Gwaram, U. A. and Abu, U. A., Evaluation of Solar Energy Potentials for Optimized Electricity Generation at Anyigba , North Central Nigeria. *Global Scientific Journals*, vol. *6*(2), pp. 263–270, 2018. https://www.worldenergy.org/wp-content/uploads/2016/10/World-Energy-Resources_SummaryReport_2016.10.03.pdf

Saleh, U A, Haruna, Y. S., & Onuigbo, F. I., *Design and Procedure for Stand-Alone Photovoltaic Power System for Ozone Monitor Laboratory at Anyigba , North Central*. vol. *4*(6), pp. 41–52, 2015.

Saleh, Umar Abubakar, Johar, M. A., Jumaat, S. A. B., Rejab, M. N., & Wan Jamaludin, W. A., Evaluation of a PV-TEG Hybrid System Configuration for an Improved Energy Output: A Review. *International Journal of Renewable Energy Development*, vol. *10*(2), pp. 385–400, 2020. https://doi.org/10.14710/ijred.0.33917

Saleh, Umar Abubakar, Johar, M. A., Jumaat, S. A. B., Rejab, M. N., & Wan Jamaludin, W. A., Evaluation of a PV-TEG Hybrid System Configuration for an Improved Energy Output: A Review. *International Journal of Renewable Energy Development*, vol. *10*(2), pp. 385–400, 2021. https://doi.org/10.14710/ijred.2021.33917

Shakeel, M., Rehman, K., Ahmad, S., Amin, M., Iqbal, N., & Khan, A., A low-cost printed organic thermoelectric generator for low- temperature energy harvesting. *Renewable Energy*, *xxxx*., 2020. https://doi.org/10.1016/j.renene.2020.11.158

Wang, X., Ting, D. S. K., & Henshaw, P., Mutation particle swarm optimization (M-PSO) of a thermoelectric generator in a multi-variable space. *Energy Conversion and Management*, vol. *224*, pp. 113387, 2020. https://doi.org/10.1016/j.enconman.2020.113387

Wen, D. L., Deng, H. T., Liu, X., Li, G. K., Zhang, X. R., & Zhang, X. S., Wearable multi-sensing double-chain thermoelectric generator. *Microsystems and Nanoengineering*, vol. *6*(1), 2020. https://doi.org/10.1038/s41378-020-0179-6

Yuan, Z., Liu, K., Xu, Z., Wang, H., Liu, Y., & Tang, X., Development of Micro-radioisotope Thermoelectric Power Supply for Deep Space Exploration Distributed Wireless Sensor Network. *Advances in Astronautics Science and Technology*, 2020. https://doi.org/10.1007/s42423-020-00062-1

Authors Biography

Engr. Umar Abubakar Saleh has a Bachelor's degree in Electrical and Electronics Engineering and a Master's degree in Electrical Engineering from ATBU, Bauchi. Umar also holds a Master's degree in Information Technology from the National Open University of Nigeria and currently doing his PhD in Electrical Engineering at the Universiti Tun Hussein Onn Malaysia in Electrical and Renewable Energy. He worked briefly with the Nigeria Television Authority (NTA) and lectured at Plateau State Polytechnic B/Ladi (2010-2011). He is currently working with the Nigerian Space Agency. He is a member of the following professional organization; IEEE, Nigerian Society of Engineers (NSE) and a registered Engineer with the Council for Regulation of Engineering in Nigeria (COREN). His research interests are in Space Engineering and Renewable Energy

Siti Amely Jumaat has been a Senior Lecturer at Universiti Tun Hussein Onn, Malaysia since 2015. She graduated from Tun Hussein Onn Institute (ITTHO-UTM) with a BSc. Honours in Electrical Engineering 2001, MEng. (Power), UTM 2004, and PhD at UiTM 2015 in Electrical Engineering. Her research interests include power and optimization systems, FACTS devices, artificial intelligence techniques, and systems for renewable energy.

Muhammad Akmal Johar is a senior lecturer at the Faculty of Mechanical and Manufacturing Engineering of Universiti Tun Hussein Onn Malaysia. He received his Bachelor's degree in 2000 from Universiti Teknologi Malaysia (UTM) in Mechatronics Engineering and his Master's degree in the same field in 2007 from the University of Applied Sciences Ravensburg-Weingarten, Germany. He obtained his PhD in Micro-Electro-Mechanical Systems from the Technical University of Kaiserslautern, Germany in 2014. His research is currently focused on developing renewable energy systems based on thermoelectric generator applications.

Wan Akasha Wan Jamaluddin received a bachelor's degree in the mechanical engineering field in 2018, pursuing various sectors. Mostly internet of things and industrial 4.0 niche, with a background in Solidworks design, different programming languages covering Arduino, MATLAB, National Instruments and Web

Development (as part of an internship experience at P2 Digital Holdings, Cyberjaya). Considered as a project-driven person with multi-role capabilities as part of his experience as a freelancer and consultant throughout bachelor degree years and currently pursuing a master's degree in the mechanical field.